Prevention and mitigation of epidemics:Biodiversity conservation and confinement policies

Emmanuelle Augeraud-Véron, Giorgio Fabbri, Katheline Schubert

Working paper GAEL n° 11/2020

GAEL
Grenoble Applied Economic Laboratory
Consumption – Energy - Innovation

Prevention and mitigation of epidemics:

Biodiversity conservation and confinement policies

Augeraud-Véron, Emmanuelle
Fabbri, Giorgio
Schubert, Katheline

October 24, 2020

JEL codes: Q56, Q57, Q58, O13, C61

https://gael.univ-grenoble-alpes.fr/accueil-gael

contact : agnes.vertier@inrae.fr

PREVENTION AND MITIGATION OF EPIDEMICS: BIODIVERSITY CONSERVATION AND CONFINEMENT POLICIES

EMMANUELLE AUGERAUD-VÉRON, GIORGIO FABBRI, AND KATHELINE SCHUBERT

ABSTRACT. This paper presents a first model integrating the relation between biodiversity loss and zoonotic pandemic risks in a general equilibrium dynamic economic set-up. The occurrence of pandemics is modeled as Poissonian leaps in economic variables. The planner can intervene in the economic and epidemiological dynamics in two ways: first (prevention), by deciding to conserve a greater quantity of biodiversity to decrease the probability of a pandemic occurring, and second (mitigation), by reducing the death toll through a lockdown policy, with the collateral effect of affecting negatively labor productivity. The policy is evaluated using a social welfare function embodying society's risk aversion, aversion to fluctuations, degree of impatience and altruism towards future generations. The model is explicitly solved and the optimal policy described. The dependence of the optimal policy on natural, productivity and preference parameters is discussed. In particular the optimal lockdown is more severe in societies valuing more human life, and the optimal biodiversity conservation is larger for more "forward looking" societies, with a small discount rate and a high degree of altruism towards future generations. Moreover, societies accepting a large welfare loss to mitigate the pandemics are also societies doing a lot of prevention. After calibrating the model with COVID-19 pandemic data we compare the mitigation efforts predicted by the model with those of the recent literature and we study the optimal prevention-mitigation policy mix.

KEY WORDS: Biodiversity, COVID-19, prevention, mitigation, epidemics, Poisson processes, recursive preferences.

JEL CLASSIFICATION: Q56, Q57, Q58, O13, C61.

Date: October 24, 2020.

1. Introduction

The hopes of the post-war period that infectious diseases were behind us thanks to control and treatment improvements (Fisher, 1995) have proved to be false: the number of emerging infectious diseases (EID) has continued to rise since the 1950s (Smith et al., 2014). The fear of a pandemic has remained vivid in the scientific community, as shown by the Clade X exercise[1] hosted at the Johns Hopkins Center for Health Security in 2018. Indeed, the number of outbreaks leading to epidemics and even pandemics has accelerated sharply over the last twenty years.

60% of these EID are caused by zoonotic pathogens, mainly (72%) of wildlife origin (Jones et al., 2008). Examples include AIDS, SARS (Severe Acute Respiratory Syndrom), MERS (Middle East Respiratory Syndrom), Nipah Virus, Avian influenza, Ebola virus and Influenza A virus subtype H1N1, as well as COVID-19. The large number of EID of zoonotic origin makes it natural to link the emergence of these diseases to the loss of biodiversity. The current COVID-19 pandemic, caused by the transmission of a pathogen from animals to humans, has put this link to the forefront of the stage.

While all the underlying mechanisms are not fully understood, a growing scientific literature documents this complex link (Morand et al., 2014, Morand, 2018). Both a dilution effect (decreasing relationship between biodiversity and EIDs, Civitello et al., 2015) and an amplification effect (increasing relationship between biodiversity and EIDs, Wood et al., 2017) are at work simultaneously (Rohr et al., 2019). The predominance of one effect over the other depends on the spatial scale at which the phenomenon is studied (Johnson et al., 2015). On a national or global scale, the dilution effect dominates (Halliday et al., 2020, Morand et al., 2014) and conserving biodiversity appears as a prevention against EIDs.

There are at least two reasons for the dilution effect (Keesing et al., 2010). Firstly, the decline in biodiversity leads to an increase in the prevalence and transmission rates at the local level and to a selection effect of the most harmful pathogenic strains. Second, habitat destruction brings species together and brings them closer to humans (Wolfe et al., 2005).[2] The promiscuity between several species, in the wild, in captivity or in breeding, increases the risk of transmission and mutation of pathogens, and makes transmission to humans more likely (LoGiudice et al., 2003).

[1] `https://www.centerforhealthsecurity.org/our-work/events/2018\_clade\_x\_exercise/`

[2] The case of bats is emblematic. Bats are reservoirs of pathogens. The reduction of their habitats due to deforestation forces them to move closer to fruit production, livestock farming and other species. See for instance Afelt et al., (2018).

The economic cost of these diseases is very high (Sands et al., 2016). The West African Ebola epidemic of 2014 led to a 10% loss of GDP in Sierra Leone and Guinea (World Bank, 2014). The COVID-19 pandemic and the policy measures adopted to fight it, that, in the absence of a vaccine or effective treatment, led to the containment of more than half of the planet during more than 2 months, resulted in severe recessions in most countries, probably the worst since the Great Depression. In the Interim Report of September 2020 of the OECD Economic Outlook (OECD, 2020) global growth is projected to -4.5% in 2020, and growth in the Euro area to -7.9%, unusually large uncertainties around these figures being acknowledged. The economic costs are direct medical costs and mostly indirect costs coming from the disruption of supply, in the industry, in the transportation sector and particularly in aviation, in the arts and entertainment sector, in the tourism sector etc.

The basic question we are interested in is whether governments, at the world level, should coordinate to invest in biodiversity conservation as a prevention policy against the risk of emerging infectious diseases, or whether they should rely on mitigation policies reducing social interactions like lockdowns once the risk materializes, or also whether they should do both. There are two levels to this question. First, a choice has to be made between investing upstream (and how much) in biodiversity conservation, at the price of an economic loss, to reduce the probability of occurrence of pandemics, or not. Second, once a pandemic hits, the severity of the mitigation policy put in place to attenuate its negative effects on health and mortality has to be decided. We design a stylized model allowing us to shed light on these issues, first from a theoretical point of view, and then with a calibration of the model to data on COVID-19 and simulations. A huge literature in economics on the COVID-19 pandemic has emerged since March 2020.[3] But the question of the links between biodiversity losses and EIDs we study here are, to the best of our knowledge, totally overlooked in this economic literature.

The theoretical framework we adopt is the one of a long-term macrodynamic economic model embedding biodiversity on the one hand, and epidemics, through a standard SIR model, on the other hand. The planner decides on the effort to be made to preserve biodiversity in order to reduce the likelihood of new EID. How much biodiversity is preserved is proportional to the size of land left undeveloped, that supports intact natural ecosystems such as primary forests. This size impacts the probability (and then the frequency) of occurrence of epidemic outbreaks. It comes at an economic cost, as land used for human activities (agricultural production, infrastructures, human settlements etc.) is a direct input in the production process.

[3]As an example, Brodeur et al. (2020) document that between March 2020 and the end of May 2020 there had been 106 NBER working papers related to COVID-19.

In addition to this risk-reducing policy, the planner also has the possibility to decide on lockdown mitigation policies in the event of a pandemic, in order to reduce population mortality, at the cost of a reduction in productive activities.

Given the simplicity of the model we can solve it explicitly. Using a social welfare function embodying society's risk aversion, aversion to fluctuations, degree of impatience and altruism towards future generations, we characterize the optimal mitigation policy and the optimal allocation of land to biodiversity conservation and study their behaviors in terms of the model's parameters.

We show that the optimal lockdown is more severe in societies valuing more human life, and that the optimal biodiversity conservation is greater in more "forward looking" societies, with a small discount rate and a high degree of altruism towards future generations. We also show that societies accepting a large welfare loss to mitigate the pandemics are also societies doing a lot of prevention, not to have to incur the loss too often and so all the more since risk aversion or the risk of pandemics absent any biodiversity are higher.

To calibrate the model we use data from Gollier (2020) on the consequences in terms of mortality and economic activity of the *laissez-faire*, a "flatten the curve" mitigation strategy and a "crush the curve", or suppression, strategy. We exhibit the terms of the trade-off between the loss of lives and the loss of GDP for the whole set of mitigation strategies, from *laissez-faire* to suppression. We compute the optimal mitigation policy as a function of the relative value the planner assigns to life over the economy, and the optimal prevention strategy, depending on the former and on the risk parameters.

The idea of assessing the economic impact of disasters that arise from "environmental" causes is the source of a well-stocked literature, both in the empirical works (see for instance Noy, 2009, and the contained references) and from the theoretical point of view (see for instance Akao and Sakamoto, 2018 or Bakkensen and Barrage, 2016). The general idea of these contributions is to understand the impact of environmental disasters on growth and development. Particularly inspiring for our research are the papers by Bretschger and Vinogradova (2016, 2019) and Douenne (2020). The latter in particular studies the possibility of dealing with disaster of endogenous probability[4] and then the idea of disaster prevention. A related contribution is the recent paper by Brock and Xepapadeas (2020) where the authors model the possible appearance of

[4]The idea of preserving biodiversity to reduce the probability of future negative outcomes is also used in another bunch of works in the literature, see for instance Baumgärtner (2007), Baumgärtner and Quaas (2010), Baumgärtner and Strunz (2014), Augeraud-Véron et al. (2019, 2020) which highlight the *insurance value* of biodiversity.

a shock linked to the arrival of an epidemic whose probability depends on the capital accumulated in the economy and the temperature anomaly caused by the use of non-renewable resources. In the present paper the focus is different since, for the first time we link biodiversity conservation, the risk of zoonotic pandemics, population and economic dynamics and mitigation policies.

The paper is organized as follows. Section 2 introduces the model's assumptions and formulation. In Section 3 we describe the explicit solution of the model. Section 4 contains numerical simulations while Section 5 concludes. All the proofs are reported in Appendices A and B.

2. The model

We consider an economy where the planner makes decisions about how to manage biodiversity and how to deal with a pandemic if it happens.

2.1. **Biodiversity and the economy.**

The planner decides at the beginning of the planning horizon how to allocate the land (whose total size is normalized to 1). A part f is devoted to biodiversity conservation while a part $1-f$ is used for various human economic activities, such as agriculture, industry, human settlement and infrastructure.

Assimilating biodiversity and land devoid of human activity f can be justified both empirically and theoretically. Empirically, the main drivers of biodiversity loss are land use change, direct exploitation of organisms, climate change, pollution and invasion of alien species (IPBES, 2019). Land use change itself is driven by agricultural expansion, the expansion of urban area (which has doubled since 1992) and the expansion of infrastructure. It has come mostly at the expense of forests. It is thus reasonable to consider the area of land that is not used for human activities f as a (proxy of a) measure of biodiversity. On the theoretical side, this is justified by the large literature on *species-area curves* describing the link between the size of a habitat and the number of species living in the same habitat. The idea, initially introduced by Arrhenius (1921) and Gleason (1922), was refined over the decades (see for instance the presentation in the book of Rosenzweig, 1995). The model can be interpreted indifferently in terms of biodiversity or in terms of habitat destruction vs conservation.

The choice of f influences the economy in two ways. Firstly in a direct way: the land devoted to human activities is used as an input in the production process. Indeed we suppose that the production is described by an aggregate production function of the form

$$Y(t) = F(1-f(t), A(t)N(t)) \tag{1}$$

where $N(t)$ is the size of the population and $A(t)$ is labor productivity at time t. We abstract in particular from the use of capital (but the model can be extended in various ways to a more general production structure). We also abstract from describing the age structure of the population. Of course this can be a very important aspect, especially in situations where the consequences of the virus in terms of severity of the disease and morbidity change consistently depending on the age of infected people, as it is the case for the COVID-19 (see for instance Salje et al., 2020).[5] The homogeneous population modeling we use cannot account for this fact. It may nevertheless be justified in a setting like ours where different viruses cause epidemics of different nature, with a different impact on age groups.

Consistently with the choice of not modeling factor accumulation and then investment, we suppose that all production is consumed:

$$C(t) = Y(t). \tag{2}$$

The second way the choice of f influences the economy is through its effects on zoonoses' outbreaks. We suppose that f influences the probability $h(t)$ that a zoonose appears and becomes a pandemic: the bigger f, the more biodiversity and the smaller the probability of epidemic outbreaks. In this sense, biodiversity conservation is a risk-reducing policy.

2.2. **Population and productivity dynamics.** The evolution of the population over time is modeled using a standard SIR model, as shown below. Absent epidemic outbreaks, population increases at a constant rate. When an epidemic outbreak hits, because of the different orders of magnitude of the parameters involved, the SIR epidemiological dynamics converges very fast in the neighborhood of the disease-free equilibrium manifold, and then is approximated by the exponential growth until either a re-emergence of the disease takes place, or a new emerging infectious disease appears. We only consider the second possibility, assuming that vaccines will prevent the disease of becoming endemic in the population.

Epidemic outbreaks are discrete events happening at time $(\tau_j)_{j\in\mathbb{N}}$. We assume that the number $\mathcal{M}_j$ of epidemic events satisfies a standard Poisson Process with instantaneous arrival rate $h(f)$. For any time t' between two events $[\tau_j, \tau_{j+1}[$, the dynamics is given by a SIR epidemic model in which population is decomposed into susceptibles S, infected I and removed R.

Population grows at rate $n = \nu - \mu$ where ν is the birth rate and μ the natural mortality rate. Total population is given at date t' by $N(t') = S(t') + I(t') + R(t')$.

[5]Macro-dynamic models which incorporate an age-structured epidemiological dynamics are for instance proposed by Acemoglu et al. (2020), Fabbri et al. (2020) and Favero et al. (2020).

The transmission rate of the disease is denoted β. The recovery rate is r. The disease-induced mortality rate is δ. The epidemiological dynamics then reads:

$$\left\{\begin{array}{l} \frac{dN(t')}{dt'} = nN(t') - \delta I(t') \\ \frac{dS(t')}{dt'} = \nu N(t') - \beta S(t') \frac{I(t')}{N(t')} - \mu S(t') \\ \frac{dI(t')}{dt'} = \beta S(t') \frac{I(t')}{N(t')} - (\delta + r + \mu) I(t') \\ \frac{dR(t')}{dt'} = rI(t') - \mu R(t') \end{array}\right. \tag{3}$$

with initial conditions $N(\tau_j) = N\left(\tau_j^-\right)$, $S(\tau_j) = N(\tau_j)$, $I(\tau_j) = I_0$ and $R(\tau_j) = 0$.

For a large variety of zoonoses, demographic parameters n, ν and μ are very small compared to epidemiological parameters β and r, and the virus-induced death rate δ is small compared to β and r. It is the case for example for COVID-19.[6] Taking into account these different orders of magnitude enables us to rewrite the dynamics at different time scales, in particular at fast time scale and at slow time scale.[8] In Lemma 2.1, we show, using the fast time scale, that the dynamics quickly converges to the disease-free equilibrium manifold (also called the slow manifold) where the number of infected I is very low (step 1). Moreover, the fast dynamics appears to be a regular perturbation of an unperturbated system with first integrals. This enables us to compute the final size of the population (Brock and Xepapadeas, 2020, Augeraud-Véron, 2020 for the COVID-19 epidemics). Step 3 of the proof explains this computation. Using slow time scale, the motion on the slow manifold is also described (step 2).

Lemma 2.1. *Following an epidemic outbreak at date τ_j, the dynamics of system (3) converges quickly to $(N(\tau_j{}^+) = kN(\tau_j), S(\tau_j{}^+) = N(\tau_j{}^+), I(\tau_j{}^+) = 0, R(\tau_j{}^+) = 0)$, where $k \in (0,1)$ depends on the transmission rate β, the duration of the disease $1/r$ and the virus-induced mortality rate δ. Then the slow motion $\frac{dN(t)}{dt} = nN(t)$, with $S(t) = N(t), I(t) = 0$ and $\frac{dR(t)}{dt} = 0$ takes place, until the next epidemic outbreak.*

Proof. The proof is given in Appendix A. □

Consequently, the population dynamics considered in the model is a growth at constant rate n between the epidemic outbreaks, interrupted by instantaneous drops of the population of size $1-k$ at each date τ when an epidemic hits:

$$\tilde{N}(\tau) = kN(\tau) \tag{4}$$

and

$$\frac{dN(t)}{N(t)} = ndt - (1-k)dq(t) \tag{5}$$

[6]For France, $n = 5.7.10^{-7}$ per day and $\mu = 2.5.10^{-5}$ per day in 2019,[7] $\beta = 0.274$, $\gamma = 0.1667$ (`http://www.data.gouv.fr`) and $\delta = 1.44.10^{-3}$ (Carcione et al., 2020).

[8]See section 4 in Augeraud-Véron and Sari (2014).

where q is a Poisson process with $\mathbb{E}[dq] = h(f)dt$, with $h'(f) < 0$: as justified above, the probability of a pandemic outbreak is all the lower since biodiversity is important.

Likewise, we assume that labor productivity grows at the exogenous and constant rate $g > 0$ between the epidemics outbreaks, and decreases instantaneously each time an epidemic hits the economy:

$$\tilde{A}(\tau) = \kappa A(\tau) \tag{6}$$

with $0 < \kappa < 1$. Thus the dynamics of productivity is described by the following stochastic differential equation:

$$\frac{dA(t)}{A(t)} = gdt - (1-\kappa)dq(t). \tag{7}$$

2.3. **Pandemics and policy response.** The transmission rate of the disease β depends on the intensity of contacts among individuals within the population: the more intense social interactions are, the larger the transmission rate. Let $e \in [0, \bar{e}]$ represent the intensity of social interactions. In normal times, this intensity is $\bar{e}$. The planner, by imposing a more or less severe and lengthy lockdown, is able to make the intensity of interactions decrease, eventually down to 0, which corresponds to a total lockdown. Therefore, the transmission rate β is a decreasing function of e. As a consequence, the instantaneous death rate $1-k$ and the share of the population still alive after an epidemic outbreak k, depend on the policy response of the planner e as well, as stated in Lemma 2.2.

Lemma 2.2. *The share of the population still alive after an epidemic outbreak, k, depends on the severity of the lockdown e. It is a function $k(e) \in (0,1)$, with $k'(e) < 0$: the more severe the lockdown is (the smaller e) the fewer deaths in the population (the larger $k(e)$).*

Proof. The proof is given in Appendix A. □

We suppose more precisely that $k(\bar{e}) = \underline{k} \in (0,1)$, $k(0) = \overline{k} \in (\underline{k}, 1)$, and $k'' \leq 0$: the marginal effectiveness of the mitigation policy is weakly decreasing (see Figure 1).

The drawbacks of the policy response to the pandemics is that it reduces labor productivity. "Non-essential" economic activities, that is activities outside the health, food and energy sectors, are stopped when teleworking is not possible.[9] Whenever it is possible, the potential issue is that it may transform from "working at home" to

[9]For instance Dingel and Neiman (2020) find that only 37% of jobs in the United States can be performed entirely at home. Bloom (2020) finds that people who are able to telework are "mostly managers, professionals, and financial workers who can easily carry out their jobs on their computers by videoconference, phone, and email."

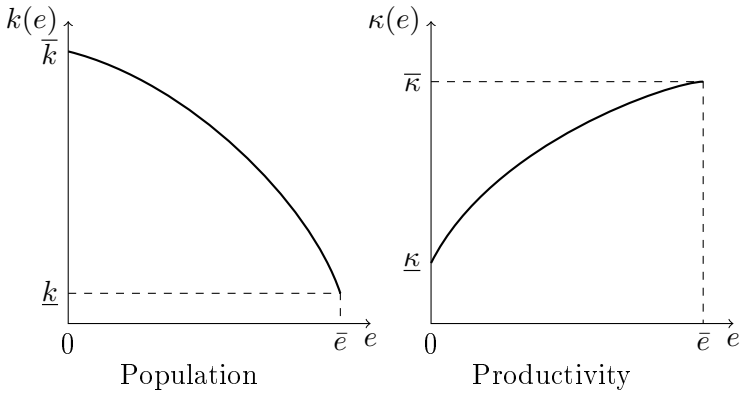

FIGURE 1. Instantaneous responses to the pandemics as a function of the mitigation policy

"shirking at home". Bloom et al. (2014) show, using an experiment performed on the 16,000 employees of a Chinese travel agency, that it is not the case: they report an increase in productivity of 13%. However, for teleworking to improve or be neutral towards productivity good working conditions at home are mandatory, like no small children to take care of simultaneously, a separate working environment, fast and reliable broadband services etc. (Bloom, 2020).

Remark that, as the papers by Ruhm (2000), Stevens et al. (2015) and Adda (2016) show, the link between economic activity and diseases is sometimes (depending on the disease) pro-cyclical. This interesting and somehow surprising pattern does not undermine our model structure where the reduction in economic activity is not exogenous but is driven by a mitigation policy aimed at reducing the death toll of the pandemics, and so where it is natural that a drop in productivity corresponds to a reduction of mortality.

According to these observations we suppose that parameter κ in equation (6) is an increasing function of e: the more severe the lockdown the larger the productivity loss. We suppose more precisely that $\kappa'(e) > 0$, $\kappa(0) = \underline{\kappa} \in (0,1)$, $\kappa(\bar{e}) = \overline{\kappa} \in (\underline{\kappa}, 1)$ and $\kappa''(e) \leq 0$ (see Figure 1).

Of course, the damages that the lockdown causes to the economy will not only come from a lower labor productivity. In particular production and supply chains will be disrupted directly, firms will get bankrupt in sectors heavily affected by the decrease of demand, etc. We make all these effects transit through a shock on labor productivity as a shortcut dictated by the fact that labor and land are the only inputs in our stylized model.

Finally, the only consequences of the lockdown policies considered here are mortality reduction on the one hand, and activity reduction through productivity losses on the other hand. However, a positive effect of the lockdown on biodiversity itself, due to reduced human pressures on wild species, has been widely observed in the case of COVID-19. The reduction in human mobility during the lockdown, relatively similar and simultaneous in a majority of countries, is unparalleled in recent history. The pressures on wildlife, and the environment in general, have been drastically reduced almost everywhere around the globe. Air quality has improved, CO_2 emissions have dropped, and there is ample anecdotal evidence of wild species thriving in these new conditions. However, this alleviation of the pressures is a short-term phenomenon, and during the recovery of the economy conditions are probably going to return to "normal". Therefore we choose not to make f depend on e.

2.4. **Social welfare.** Choosing a social utility functional is delicate since population ethics is a difficult matter (see for instance Arrhenius et al., 2017). We consider here a class of social welfare functions parameterized by $\lambda \in [0,1]$ by supposing that the planner's instantaneous utility at time t is of the form

$$N(t)^{\lambda} u\left(\frac{C(t)}{N(t)}\right)$$

where $u\left(\frac{C(t)}{N(t)}\right)$ is the utility derived from per-capita consumption. The value of λ measures the degree of altruism towards individuals of future cohorts (see for instance *e.g.* Boucekkine et al., 2014) and it can be justified, as done by Barro and Becker (1989) in a model of endogenous fertility choice by the "impure altruism" of parents. The two polar cases $\lambda = 0$ and $\lambda = 1$ correspond respectively to standard average utilitarianism and total utilitarianism.

The planner maximizes a non-separable intertemporal utility *à la* Epstein-Zin-Weil, supposing that agents' preferences are characterized by a constant relative risk aversion $\theta > 0$ (and $\theta \neq 1$), an intertemporal elasticity of substitution $1/\phi > 0$ (ϕ represents aversion to fluctuations) and a discount rate $\rho > 0$.

We can dig a little deeper in the utility functional to understand which choices of parameters are meaningful. If we look at the analogous of the informal representation of preferences given for instance by Svensson (1989) (see also Augeraud-Véron et al.,

2019) in our case, we have,[10] for given controls $e(t)$ and $f(t)$,

$$U(t) = \frac{1}{1-\phi} N(t)^{\lambda} \left(\frac{C(t)}{N(t)} \right)^{1-\phi} + e^{-\rho \mathrm{d}t} \left(\mathbb{E}_t \left[U(t+\mathrm{d}t)^{\frac{1-\theta}{1-\phi}} \right] \right)^{\frac{1-\phi}{1-\theta}}. \tag{8}$$

With this CRRA specification of the utility derived from per capita consumption we have to impose $\phi \in (0,1)$ to make sure that the planner values positively an increase of the population.

3. The optimal policy

In order to explicitly solve the problem we specify the described setting by considering a linear probability of pandemics and a linear production function.

The instantaneous arrival rate of the Poisson process is then:

$$h(f) \quad = \quad \varepsilon(1-f), \qquad \varepsilon \in (0,1].$$

We acknowledge that this specification is not entirely satisfactory. Damages, in terms of occurrence of epidemic outbreaks, caused by the destruction of biodiversity would be better modeled as convex, or even better as featuring discontinuities and tipping points. We stick to this linear specification in order to obtain close-form solutions.

The production function reads:

$$Y(t) = (1-f(t))A(t)N(t).$$

Then per-capita consumption is :

$$\frac{C(t)}{N(t)} = (1-f(t))\, A(t)$$

and the instantaneous utility function becomes:

$$\frac{1}{1-\phi} N(t)^{\lambda} \left(\frac{C(t)}{N(t)} \right)^{1-\phi} = \frac{1}{1-\phi} N(t)^{\lambda} \left(1-f(t)\right) A(t))^{1-\phi}.$$

Observe that, abstracting from dynamics effects, at the level of the instantaneous utility function, per-capita consumption does not decreases when N increases so no "quality/quantity" trade-off takes place. This is due to the linear specification of the production function.

[10] As clarified by Epaulard and Pommeret (2003) (see in particular equation (2.1) and Footnote 2) this expression is equivalent to the one originally proposed by Svensson via a transformation *à la* Duffie and Epstein (1992).

All in all the HJB equation of the problem reads:

$$\rho\frac{1-\theta}{1-\phi}V(A,N)=\max_{f,e}\left[N^{\lambda}\frac{[(1-f)A]^{1-\phi}}{1-\phi}\frac{1}{((1-\theta)V(A,N))^{\frac{1-\phi}{1-\theta}-1}}\right.$$
$$\left.+V_A gA+V_N nN+\varepsilon(1-f)\left(V(\kappa(e)A,k(e)N)-V(A,N)\right)\right] \tag{9}$$

Theorem 3.1. *Suppose that the function of the variable* $e\in[0,\bar{e}]$

$$k(e)^{\frac{\lambda}{1-\phi}}\kappa(e) \tag{10}$$

has a unique maximum point of $e^*\in[0,\bar{e}]$*. Suppose that the following interior condition*

$$\rho>(1-\phi)g+\lambda n \tag{11}$$

is verified together with the following transversality condition:

$$(1-\theta+\phi)\rho>\frac{1-\theta}{1-\phi}\left((1-\phi)g+\lambda n\right). \tag{12}$$

Then optimal policy $(f^*(\cdot),e^*(\cdot))$ *is deterministic and constant and it is given by* $e^*(\cdot)\equiv e^*$ *and* $f^*(\cdot)\equiv f^*$ *defined by:*[11]

$$f^*:=1-\min\left[1,\frac{\rho-(1-\phi)g-\lambda n}{\phi\varepsilon}\frac{1-\theta}{1-\left(k(e^*)^{\frac{\lambda}{1-\phi}}\kappa(e^*)\right)^{1-\theta}}\right]. \tag{13}$$

The corresponding social welfare is given by

$$V(A,N)=X\frac{\left(N^{\frac{\lambda}{1-\phi}}A\right)^{1-\theta}}{1-\theta}$$

with

$$X=\left(\frac{\phi^{\frac{\phi}{1-\phi}}(1-\theta)}{(\rho-(1-\phi)g-\lambda n)^{\frac{\phi}{1-\phi}}\varepsilon\left[1-\left(k(e)^{\frac{\lambda}{1-\phi}}\kappa(e)\right)^{1-\theta}\right]}\right)^{1-\theta} \tag{14}$$

Proof. See Appendix B. □

Theorem 3.1 first allows us to learn about the optimal mitigation policy. Denote by $z(e)$ the function of e defined in equation (10). With our assumptions on the functions k and κ, $z(e)$ is a positive and concave function of e: $z''(e)\leq 0$.

[11] Observe that, since $\kappa(e),k(e)\in(0,1)$ then the term $(1-\theta)\left[1-\left(k(e^*)^{\frac{\lambda}{1-\phi}}\kappa(e^*)\right)^{1-\theta}\right]^{-1}$ is positive for any choice of $\theta>0$.

If $z'(e) < 0$ for all $e \in [0, \bar{e}]$, the maximum of z is attained for $e = 0$. The optimal policy is total lockdown: $e^* = 0$. The condition $z'(e) < 0$ is equivalent to $\frac{\lambda}{1-\phi}\frac{k'(0)}{k(0)} + \frac{\kappa'(0)}{\kappa(0)} < 0$, that is $-\frac{\kappa'(0)/\kappa(0)}{k'(0)/k(0)} < \frac{\lambda}{1-\phi}$. Denote $\overline{\tau} := -\frac{\kappa'(0)/\kappa(0)}{k'(0)/k(0)}$. The case under study is then relevant for $\frac{\lambda}{1-\phi} > \overline{\tau}$, that is for large values of the society's relative preference for life. Symmetrically, if $z'(e) > 0$ for all $e \in [0, \bar{e}]$, the maximum of z is attained for $e = \bar{e}$ and the optimal policy is no lockdown: $e^* = \bar{e}$. This case is relevant for $\frac{\lambda}{1-\phi} < \underline{\tau}$, where $\underline{\tau} := -\frac{\kappa'(\bar{e})/\kappa(\bar{e})}{k'(\bar{e})/k(\bar{e})}$, that is for small values of the relative preference for life. Finally, the optimal mitigation policy is interior for values of the relative preference for life between $\underline{\tau}$ and $\overline{\tau}$. e^* is then given by the first order condition for the maximization of (10):

$$-\frac{\kappa'(e)/\kappa(e)}{k'(e)/k(e)} = \frac{\lambda}{1-\phi}. \tag{15}$$

If the pandemic occurs the planner will react instantaneously by no/partial/total lockdown, according to her relative preference for life over the economy $\frac{\lambda}{1-\phi}$, and the shape of the k and κ loss functions. On the left side of equation (15) we can recognize the opposite of the ratio between the elasticities of κ and k with respect to e. This expression can also be rewritten as $-(1-\phi)\kappa'(e)/\kappa(e) = \lambda k'(e)/k(e)$. Unsurprisingly in this expression the contribution of the elasticity of the negative effect on the population is weighted with λ. Indeed, as already mentioned, the per-capita consumption is not affected by the shock and the negative effect of the population loss only comes through the term N^λ appearing in the utility function. This underlines once more the role of λ as a measure of the value of a life in the planner functional. Similarly the shock on productivity is weighted by the exponent $(1-\phi)$ of the productivity in the instantaneous utility. Risk aversion plays no role here. This is not particularly surprising because the choice of e has some impact on the system only after (and if) the shock occurs. Conversely the value of θ clearly appears in the choice of f which is the "disaster prevention choice" of the planner. Due to the linearity of the model, the growth rates of the productivities (*i.e.* g and n) do not enter in the choice of e.

Turning to the biodiversity conservation policy, we obtain several results by inspection of equation (13).

First, the share of land optimally devoted to biodiversity conservation is a decreasing function of the discount rate: the more the planner is interested in future outcomes, the more she wants to reduce the risk of pandemic outbreaks and the more biodiversity is needed. Conversely the higher the inherent capacity of the system to regenerate after a shock (measured by the deterministic growth rates of the productivity and the population g and n) the smaller the optimal biodiversity conservation.

Then, the role of the parameter ε describing the relationship between biodiversity and the probability of a pandemic is straightforward; a larger ε leads to more biodiversity conservation, which is conform to intuition. Indeed, the larger ε the more powerful is biodiversity conservation in terms of risk reduction.

As for the preference parameters the results are not obvious and are collected in the following proposition.

Proposition 3.2. *Suppose that the hypotheses of Theorem 3.1 are verified and that the optimal value of f^* is interior. Then f^* is an increasing function of θ and λ. Moreover it is an increasing function of ϕ when the discount rate is high enough: $\rho \geq g + \lambda n$.*

Proof. See Appendix B. □

Even if it is not obvious at a first look the impact of risk aversion is conform to intuition: f^* is an increasing function of risk aversion, meaning that the more risk averse the planner is, the more she wants to reduce the risk of future pandemics.

Similarly Proposition 3.2 tells us that f^* is an increasing function of λ.

We can dig a bit further here. In the limit case of average utilitarianism ($\lambda = 0$), the optimal mitigation policy is no lockdown ($e^* = 0$), since $\frac{\lambda}{1-\phi} = 0 < \underline{\tau}$. But is it necessarily the case that the optimal biodiversity conservation is nil? We have:

$$f^* \,|_{\lambda=0} = 1 - \min\left[1, \frac{\rho - (1-\phi)g}{\phi} \frac{1-\theta}{1-\overline{\kappa}^{1-\theta}}\right] \tag{16}$$

If the productivity loss absent any social distancing is very small, $\overline{\kappa}$ is close to 1 and $f^* = 0$: there is no biodiversity conservation. Conversely, if the pandemic causes a significant productivity loss even without lockdown (and not only loss of lives), conserving some biodiversity may be optimal to reduce the risk of pandemic outbreaks.

Moreover, we can infer from the previous results the nature of the links between optimal prevention and optimal mitigation. At the beginning of the planning horizon, the planner chooses the optimal mitigation policy she will put in place each times a pandemic hits. This policy is all the more severe since she values life a lot. Therefore, the loss she incurs each time a pandemic hits, $1 - k(e*)^{\frac{\lambda}{1-\phi}}\kappa(e^*)$ is all the larger (see the proof of Proposition 3.2). To avoid paying this large cost too often, the planner will choose to conserve a lot of biodiversity.

Finally Proposition 3.2 emphasizes that f^* is an ambiguous function of the aversion to fluctuations ϕ but a sufficient condition for f^* being an increasing function of aversion to fluctuations is that the discount rate is high enough: $\rho \geq g + \lambda n$. In the case of average utilitarianism ($\lambda = 0$), this condition reads $\rho > g$ and is necessary and sufficient.

Indeed we have, using equation (16) when the solution is interior:

$$\frac{\partial f^*}{\partial \phi} |_{\lambda=0} = \frac{1-\theta}{1-\overline{\kappa}^{1-\theta}} \frac{\rho - g}{\phi^2}.$$

where the term $\frac{1-\theta}{1-\overline{\kappa}^{1-\theta}}$ is positive for any choice of θ since $\kappa \in (0,1)$.

Corollary 3.3. *Let hypotheses of Theorem 3.1 be satisfied. Then the optimal evolution of $A(t)$ and $N(t)$ are*

$$\begin{aligned} A(t) &= A_0 e^{gt} \kappa(e^*)^{q(t)-q(0)} \\ N(t) &= N_0 e^{nt} k(e^*)^{q(t)-q(0)} \end{aligned}$$

where the increment $q(t)-q(0)$, that is the number of pandemic outbreaks since date 0, is Poisson-distributed with mean $\varepsilon(1-f^*)$. In particular

$$\mathbb{E}(A(t)) = A_0 e^{(g-\varepsilon(1-f^*)(1-\kappa(e^*)))t}, \quad Var(A(t)) = (\mathbb{E}(A(t)))^2 \left(e^{(g-\varepsilon(1-f^*)(1-\kappa(e^*)))t} - 1\right)$$

$$\mathbb{E}(N(t)) = N_0 e^{(n-\varepsilon(1-f^*)(1-k(e^*)))t}, \quad Var(N(t)) = (\mathbb{E}(N(t)))^2 \left(e^{(n-\varepsilon(1-f^*)(1-k(e^*)))t} - 1\right)$$

The expressions of previous corollary are particularly transparent: the evolution of $A(t)$ and $N(t)$ only depends on their pandemic-free (exponential) dynamics and on the size and the number of shocks (which, in the model, always have the effect of reducing the quantities by the same factor). The growth rates of the expected productivity and population are equal to the pandemic-free growth rates (g and n respectively) adjusted for the effects of possible pandemics given by the size of the loss weighted by the probability of the pandemics. A large weight of life in the social welfare function (large λ) causes a severe optimal mitigation policy (small e^*) and thus a large drop of productivity and a small death toll, together with an important risk-reducing effort of biodiversity conservation (large f^*). Therefore, the growth rate of the expected population is unambiguously an increasing function of λ, whereas the effect of λ on the growth rate of expected productivity is ambiguous.

4. Numerical illustration

4.1. **Specifications.** We use the following specifications for the k and κ functions:

$$\begin{aligned} k(e) &= \overline{k} - \left(\overline{k} - \underline{k}\right) \left(\frac{e}{\overline{e}}\right)^a \\ \kappa(e) &= \underline{\kappa} + \left(\overline{\kappa} - \underline{\kappa}\right) \left(\frac{e}{\overline{e}}\right)^b \end{aligned}$$

When $a \geq 1$ and $0 < b \leq 1$ these specifications satisfy the assumptions made above.

		Gollier	Greenstone and Nigam	Thurnström et al.
Laisser-faire	mortality (% population)	0.54	1.13	0.68
	economic cost (% GDP)	3.73		2
Mitigation	mortality (% population)	0.363	0.52	0.29
	economic cost (% GDP)	5.74		6.2
Suppression	mortality (% population)	0.029		
	economic cost (% GDP)	13.53		

TABLE 1. Data

4.2. **Data.** Gollier (2020) calibrates a SIR model on the COVID-19 pandemic data for France and performs cost-benefit analysis exercises. He estimates the death toll and the GDP loss in the no-policy case, and for two strategies in particular: the "suppression", or "crush the curve" strategy, consisting in confining 90% of the population for 4 months to eradicate the virus, and the "flatten-the-curve" strategy, consisting in confining 30% of the population for 5 months. We use these data for our benchmark calibration.

Needless to say, the parameters used by Gollier to calibrate the SIR model and the results he obtains are highly uncertain. We report in Table 1 Gollier's results and also the results of two other papers, obtained for different countries and with different methods, to assess whether they give similar or very different information.

Greenstone and Nigam (2020) are only interested in the death toll of the pandemic. Using the famous Ferguson et al. (2020) simulation model of COVID-19's spread and mortality impacts in the United States, they estimate the death toll in the *laissez-faire* situation and in the case of a moderate social distancing policy, taking into account, as Gollier does, not only direct deaths but also the deaths due to the overwhelming of hospital intensive care units. Thunström et al. (2020) also examine the impacts of social distancing in the US, but on both the death and the GDP sides. They use epidemiological and economic forecasting to perform a cost–benefit analysis of controlling the COVID-19 outbreak. We assume here that Gollier's "flatten the curve" scenario, Greenstone and Nigam "moderate social distancing" scenario and Thunström et al. "control"

	$k(e)$	$\kappa(e)$
laissez-faire	$\underline{k} = 1 - 0.0054$	$\overline{\kappa} = 1 - 0.0373$
mitigation	$\overline{k} - \left(\overline{k} - \underline{k}\right) e_m^a = 1 - 0.00363$	$\underline{\kappa} + \left(\overline{\kappa} - \underline{\kappa}\right) e_m^b = 1 - 0.0574$
suppression	$\overline{k} = 1 - 0.00029$	$\underline{\kappa} = 1 - 0.1353$

TABLE 2. Calibration of the loss functions

scenario are roughly equivalent in terms of severity and length of the lockdown. Table 1 shows that Gollier and Thunström et al. give similar estimates of the death toll in the *laissez-faire* scenario (no policy) and the mitigation (flatten the curve) scenario whereas Greenstone and Nigam are more pessimistic. For the economic cost of the pandemic in terms of GDP loss, the results from Thunström et al. we report in the table correspond to immediate losses (the year of the outbreak). The authors also compute the present value of GDP losses on a 30-year horizon, that we do not use for comparability with Gollier's estimates. Gollier is more pessimistic in the *laissez-faire* scenario, less so in the mitigation scenario. But again theses estimates are very uncertain.

4.3. **Calibration.** We normalize $\bar{e}$ to 1.

We use Gollier's data, as reported in Table 1, to calibrate the parameters of the k and κ loss functions. The *laissez-faire*, mitigation and suppression scenarios correspond respectively to $e = \bar{e} = 1$, $e = e_m$ unknown and $e = 0$. We have to calibrate parameters $\underline{k}$, $\overline{k}$, $\underline{\kappa}$, $\overline{\kappa}$, e_m, a and b. The relationships reported in Table 2 allow us to obtain 6 out of these 7 parameters. We choose to calibrate a/b, set arbitrarily $a = 2$ and deduce b. The results are in Table 3.

$\bar{e}$	e_m	a	b	$\underline{k}$	$\overline{k}$	$\underline{\kappa}$	$\overline{\kappa}$	ρ	g	n	ϕ
1	0.753	2	0.8	0.9946	0.99971	0.8647	0.9627	0.02	0.02	0.005	0.95

TABLE 3. Results of the calibration of the loss functions, and other parameters

We obtain that the mitigation strategy corresponds to a moderate lockdown: social interactions are reduced by around one quarter ($e_m = 0.753$).

The other parameters of the model, namely the discount rate ρ, the deterministic growth rates of population and productivity n and g, and the aversion to fluctuations ϕ are in the range of the parameters found in the literature (Table 3).

4.4. **Results.** Figure 2 shows the terms of the raw trade-off between the loss of lives and the loss of GDP, for a mitigation strategy between 0 (suppression), on the left end

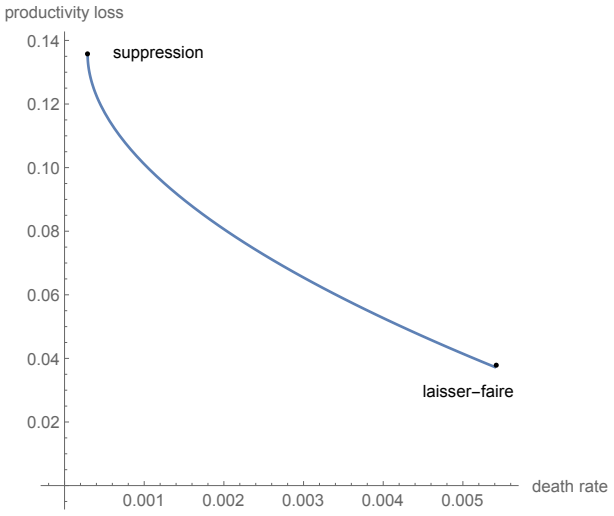

FIGURE 2. Trade-off lives vs economy

of the curve, and $\bar{e}$ (*laissez-faire*), on the right end. This trade-off is monotonous, in contrast to what Acemoglu et al. (2020) obtain in a model with several age classes. In their case, if, from the *laissez-faire* situation, the planner decides to confine the older age classes, most at risk, then she can at the same time save lives and mitigate the GDP loss. For more severe mitigation policies, all age classes are confined and the trade-off becomes similar to ours.

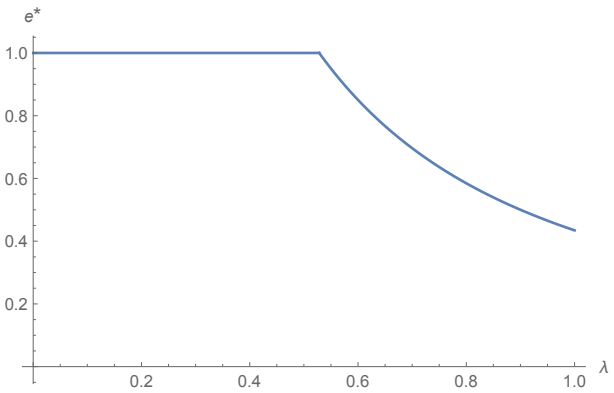

FIGURE 3. Optimal mitigation policy as a function of λ

Figure 3 shows the optimal mitigation policies as a function of λ. With our specifications and calibration, the thresholds of $\lambda/(1-\phi)$ under which there is no mitigation and above which there is suppression are respectively $\underline{\tau} = 10.5672$ and $\overline{\tau} = +\infty$. With

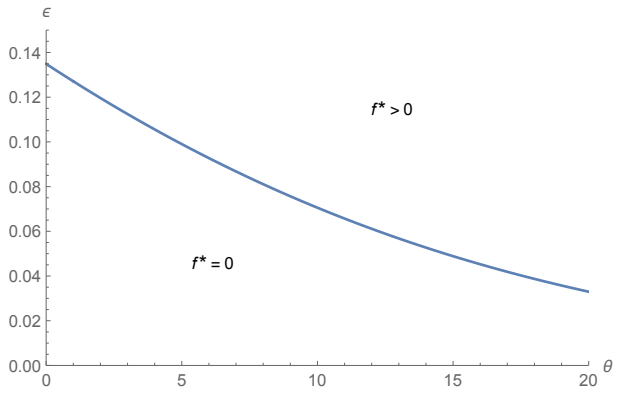

FIGURE 4. $(\theta - \varepsilon)$ frontier for $\lambda = 0.9$

$\phi = 0.95$, the lower threshold corresponds to $\lambda = 0.52$. In the case of average utilitarianism ($\lambda = 0$) and for all $\lambda < 0.52$ it is not optimal to engage in mitigation. In the case of total utilitarianism ($\lambda = 1$) we obtain $e^* = 0.44$: optimal mitigation is far more severe that in Gollier (2020)'s mitigation strategy for which $e^* = e_m = 0.753$, that is far more severe than the the "flatten-the-curve" strategy, consisting in confining 30% of the population for 5 months.

The very recent literature on the cost-benefit analysis of COVID-19 mitigation policies commonly uses the Value of a Statistical Life (VSL) to monetize the death toll and compare the benefits of the policy in terms of avoided deaths to its costs in terms of foregone GDP. We do not need to do that here. In our model, the relative value of life is $\frac{V_N N}{V_A A}$, the value of the population over the value of productivity, population and productivity being both valued at the marginal increase of welfare their increase causes. With our specifications the relative value of life is constant and equal to $\frac{\lambda}{1-\phi}$. It only depends on the characteristics of the social welfare function, the degree of partial altruism λ and the aversion to fluctuations ϕ.

The optimal biodiversity conservation f^*, given by equation (13), depends on all the parameters identified above but also on the risk parameters, the risk aversion θ and the probability that the pandemic hits absent biodiversity ε. This last parameter is particularly difficult to calibrate. Instead of engaging in the exercise, we choose to determine the couples (θ, ε) constituting the frontier between no biodiversity conservation and biodiversity conservation or, to put things differently, no prevention and prevention of the pandemics. This frontier is represented on Figure 4 for $\lambda = 0.9$. We see that with our calibration, when risk aversion is around 2 biodiversity conservation becomes optimal for very high values of the probability of pandemics (around 12%), whereas when

risk aversion is around 20 it becomes optimal for values of the probability of pandemics around 4%. Again, these figures are only illustrative.

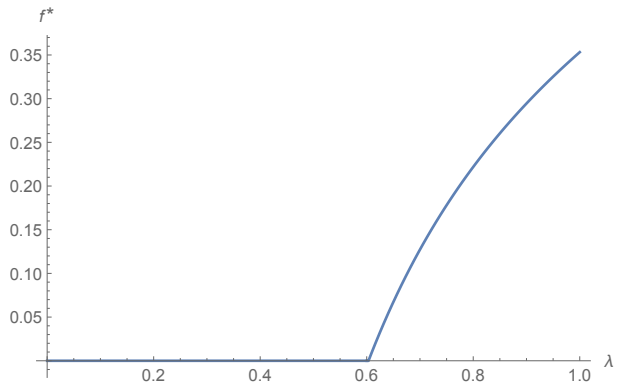

FIGURE 5. Optimal prevention policy as a function of λ, for $\varepsilon = 0.05$ and $\theta = 8$

To compute the optimal prevention policy as a function of λ we choose $\theta = 10$ and $\varepsilon = 0.1$. Figure 5 shows that there is no biodiversity conservation until $\lambda = 0.6$, and that in the case of total utilitarianism 35% of the land is devoted to biodiversity conservation for the prevention of pandemics.

5. Conclusion

Following the outbreak of the COVID-19 pandemic a long series of contributions in theoretical and applied economics have been published.

In this work we dig a little not only into the policies to be implemented to mitigate the effects of the pandemic when it occurs, but also (and above all) into one of the possible vectors to prevent it. We propose, for the first time as far as we know, a theoretical dynamic model that looks, in the case of a stylized economy, at the economic importance of reducing the likelihood of zoonotic outbreaks through the conservation of biodiversity.

We consider a family of instantaneous utility functions admitting per capita consumption and the size of the population as arguments, to be able to derive from preferences the choice society has to make between economic activity and lives' preservation when an epidemic outbreak happens.

Despite a certain technical complexity (due to the presence of jump processes and of an Epstein-Zin type social welfare functional) the model is completely solved and a discussion about the impact of various elements at stake (situation of the natural environment, productivity, preferences) is developed.

Emphasizing a role of "forward looking" instrument, we prove that biodiversity conservation is more important when the social welfare functional is characterized by a lower discount rate and a stronger degree of altruism towards individuals of future cohorts. Not surprisingly, given the risk-reducing (prevention) effect of biodiversity in the model, biodiversity conservation is also more relevant when the risk aversion or the risk of pandemics are higher.

After calibrating the model using the data from Gollier (2020) we exhibit the terms of the trade-off between the loss of lives and the loss of GDP for the whole set of mitigation strategies, from *laissez-faire* to suppression.

In this first attempt to look, in a macrodynamic model, at the economic consequences of the effects of the destruction of biodiversity on the probability of developing zoonoses, we considered the problem in a simplified setting that allow us in particular to obtain an explicit solution to the optimization problem. We believe that the essential features of the problem and the essential trade-offs are maintained in this formulation. There remain, however, very relevant aspects of the problem that cannot be described in our set-up. They could be interesting extension of our research.

First, we have already mentioned the absence of age structure of the population in the model, which is certainly an element of interest in the case of zoonoses that, as in the case of COVID-19, have a very different impact on different age groups and then on the best policies to be implemented (see for instance Acemoglu et al., 2020).

Secondly, capital accumulation is absent in our model. Taking it into account would make the effects of containment policies persistent, as the decrease of labor productivity, causing a decrease of GDP, would lead to less capital accumulation, which would have long-lasting consequences (see Brock and Xepapadeas, 2020). Moreover, the epidemics could cause capital destruction, if activities disappear permanently because of a permanent change of the demand pattern.

Then, our model describes the world economy, and is unable to take into account globalization and the role of trade and travels in the spread of epidemics and the fact that they become pandemics (Tatem et al., 2006).

Another element of interest that has been particularly highlighted during the COVID-19 outbreak is the differential effect of containment measures (and in particular lockdown) on different sectors of the economy, with different impact on productivity of different sectors and reallocation effects (see for example Krueger et al., 2020). The food and agriculture sector could take the crisis as an opportunity to accelerate its transformation towards more resilience, which could at the same time improve its productivity and decrease its pressure on the environment. The crises produces strong incentives for more robots and digital technologies in industrial sectors, which has the

potential to improve productivity. Besides, innovation may be boosted, through a creative destruction process. However, the long term perspectives are still unclear. These sectoral effects and their consequences on long term growth and innovation cannot be taken into account in a one-sector set-up as the one we consider here.

Finally, another important shortcoming of our analysis is that distributive issues are absent. The COVID-19 crisis has affected very differently people according to their age, but also to their income level. The differential effect across income categories is the addition of a direct effect (richer people have better access to the health system, live in larger houses and a less polluted environment, and are better protected against unemployment and the loss of their income) and an indirect effect through public policies (the lockdown affects more the jobs of poorer people), the poorest being more affected.[12]

The stylized framework we have developed in this work would enable us to extend our research in several directions. First, introducing capital accumulation and considering more general production functions is clearly on he agenda. Second, we intend to consider a game-theoretical extension of the model to study the cost of non-coordination of policies at the world level. Finally, we would like to consider uncertainty, disentangling aversion to ambiguity, risk aversion and aversion to fluctuations. Indeed, the COVID-19 crisis has made clear how little we know on the biological and epidemiological sides, and also on the side of the appropriate mitigation policies.

References

Acemoglu, D., Chernozhukov V., Werning, I. and Whinston, M. (2020). A multi-risk SIR model with optimally targeted lockdown, NBER WP 27102.

Adda, J. (2016). Economic activity and the spread of viral diseases: Evidence from high frequency data. The Quarterly Journal of Economics, 131(2), 891-941.

Afelt, A., Frutos, R., and Devaux, C. (2018). Bats, coronaviruses, and deforestation: Toward the emergence of novel infectious diseases?. Frontiers in microbiology, 9, 702.

Akao, K.-I. and Sakamoto, H. (2018) A theory of disasters and long-run growth. Journal of Economic Dynamics and Control, 95:89-109.

Arrhenius, O. (1921). Species and Area. Journal of Ecology 9:95–99.

Arrhenius, G., Ryberg, J. and Tännsjö, T. (2017). The Repugnant Conclusion, Stanford Encyclopedia of Philosophy.

[12]For a summary of theses effects see World Bank (2020). For an analysis see Hacioglu et al. (2020) and O'Donoghue et al. (2020).

Augeraud-Véron, E., and Sari, N. (2014). Seasonal dynamics in an SIR epidemic system. Journal of mathematical biology, 68(3), 701-725.

Augeraud-Véron, E., Fabbri, G., and Schubert, K. (2019). The value of biodiversity as an insurance device. American Journal of Agricultural Economics, 101(4), 1068–1081.

Augeraud-Véron, E., Fabbri, G. and Schubert, K., (2020). Volatility-Reducing Biodiversity Conservation Under Strategic Interactions. Preprint (No. 2020011). Université Catholique de Louvain, Institut de Recherches Economiques et Sociales (IRES).

Augeraud-Véron, E. (2020). Lifting the COVID-19 lockdown: different scenarios for France. Mathematical Modelling of Natural Phenomena, 15, 40.

Bakkensen, L. and Barrage, L. (2016). Do disasters affect growth? A macro model-based perspective on the empirical debate. Working paper, Brown University.

Barro, R. and Becker, G. (1989). Fertility Choice in a Model of Economic Growth. Econometrica, 57(2), 481–501.

Baumgärtner, S. (2007). The insurance value of biodiversity in the provision of ecosystem services. Natural Resource Modeling 20(1), 87-127.

Baumgärtner, S., and Quaas, M. F. (2010). Managing increasing environmental risks through agrobiodiversity and agrienvironmental policies. Agricultural Economics, 41(5), 483-496.

Baumgärtner, S. and Strunz, S. (2014). The economic insurance value of ecosystem resilience. Ecological Economics 101, 21-32.

Bloom, N., Liang, J., Roberts, J., Zhichun, J.Y. (2014), Does Working from Home Work? Evidence from a Chinese Experiment. Quarterly Journal of Economics, 130(1), 165–218.

Bloom, N (2020), How working from home works out. Policy brief, Institute for Economic Policy research, Stanford University, June.

Boucekkine, R., Fabbri, G. and Gozzi, F. (2014). Egalitarianism under population change: age structure does matter. Journal of Mathematical Economics, 55, pp.86-100.

Bretschger, L., and Vinogradova, A.(2016). Escaping Damocles' Sword: Endogenous Climate Shocks in a Growing Economy. Working Paper, ETH Zurich.

Bretschger, L., and Vinogradova, A. (2019). Best policy response to environmental shocks: Applying a stochastic framework. Journal of Environmental Economics and Management, 97, 23-41..

Brock, W., and Xepapadeas, A. (2020). The economy, climate change and infectious diseases: links and policy implications. Environmental and Resource Economics, 1-14.

Brodeur, A., Gray, D. M., Islam, A. and Jabeen Bhuiyan, S. (2020), A Literature Review of the Economics of COVID-19. IZA Discussion Paper 13411.

Carcione, J. M., Santos J. E., Bagaini C. and Ba J. (2020). A Simulation of a COVID-19 Epidemic Based on a Deterministic SEIR Model. Frontiers in Public Health, 8:230

Civitello, D. J., Cohen, J., Fatima, H., Halstead, N. T., Liriano, J., McMahon, T. A., ... & Rohr, J. R. (2015). Biodiversity inhibits parasites: broad evidence for the dilution effect. Proceedings of the National Academy of Sciences, 112(28), 8667-8671

Dingel, J. and Neiman, B. (2020), How Many Jobs Can be Done at Home?. Covid Economics 1, 16-24.

Douenne, T. (2020), Disaster risks, disaster strikes, and economic growth: The role of preferences. Review of Economic Dynamics, 38, 251–272.

Duffie, D. and Epstein, L. G. (1992). Stochastic differential utility. Econometrica, 60(2), 353–94.

Epaulard, A. and Pommeret, A. (2003). Optimally eating a stochastic cake: a recursive utility approach. Resource and Energy Economics, 25(2), pp.129-139.

Fabbri, G., Gozzi, F., and Zanco, G. (2020). Verification Results for Age-Structured Models of Economic-Epidemics Dynamics. arXiv preprint arXiv:2008.07335.

Favero, C. A., Ichino, A. and Rustichini, A., 2020. Restarting the economy while saving lives under Covid-19. CEPR Discussion Papers 14664.

Ferguson, N. M. et al. (2020). Impact of non-pharmaceutical interventions (NPIs) to reduce COVID-19 mortality and healthcare demand. London: Imperial College COVID-19 Response Team.

Fisher, J. A. (1995). The plague makers. JAMA, 274(7), 537-537.

Gleason, H. A. (1922), On the relation between species and area. Ecology 3, 158–162.

Gollier, C. (2020). Cost-benefit analysis of age-specific deconfinement strategies. Covid Economics, 24, 1–29.

Greenstone, M. and Nigam, V. (2020). Does social distancing matter? Covid Economics, 7, 1–23.

Hacioglu, S., Känzig, D. and Surico, P. (2020)„ The distributional impact of the pandemic, Discussion Paper DP15101, Centre for Economic Policy Research, July 26.

Intergovernmental Science-Policy Platform on Biodiversity and Ecosystem Services (IPBES. (2019). Summary for Policymakers of the Global Assessment on Biodiversity and Ecosystem Services (IPBES). https://ipbes.net/news/ipbes-global-assessment-summary-policymakers-pdf

Jones, K.E. Patel, N.G., Levy, M.A., Storeygard, A., Balk, D., Gittleman, J.L. and Daszak, P. (2008). Global Trends in Emerging Infectious Diseases. Nature, 452, 990-994.

Johnson, P. T., Ostfeld, R. S., and Keesing, F. (2015). Frontiers in research on biodiversity and disease. Ecology letters, 18(10), 1119-1133.

Halliday, F. W., Rohr, J. R., and Laine, A. L. (2020). Biodiversity loss underlies the dilution effect of biodiversity. bioRxiv.

Keesing, F., Belden, L. K., Daszak, P., Dobson, A., Harvell, C. D., Holt, R. D. and Myers, S. S. (2010). Impacts of biodiversity on the emergence and transmission of infectious diseases. Nature, 468(7324), 647-652.

Krueger, D., Uhlig, H., and Xie, T. (2020). Macroeconomic dynamics and reallocation in an epidemic. NBER working paper 27047.

LoGiudice, K., Ostfeld, R. S., Schmidt, K. A., & Keesing, F. (2003). The ecology of infectious disease: effects of host diversity and community composition on Lyme disease risk. Proceedings of the National Academy of Sciences, 100(2), 567-571.

Morand, S., Jittapalapong, S., Suputtamongkol, Y., Abdullah, M. T. and Huan, T. B. (2014). Infectious diseases and their outbreaks in Asia-Pacific: biodiversity and its regulation loss matter. PLoS One, 9(2).

Morand, S. (2018). Biodiversity and disease transmission. In The Connections Between Ecology and Infectious Disease (pp. 39-56). Springer, Cham.

Noy, I (2009). The macroeconomic consequences of disasters. Journal of Development Economics, 88:221-231.

O'Donoghue, C., Sologon, D. M., Kyzyma, I. and McHale, J. (2020), Modelling the Distributional Impact of the COVID?19 Crisis, Fiscal Studies, 41(2), 321–336.

OECD, (2020). Economic Outlook, June 2020.

Rohr, J. R., Civitello, D. J., Halliday, F. W., Hudson, P. J., Lafferty, K. D., Wood, C. L., & Mordecai, E. A. (2019). Towards common ground in the biodiversity–disease debate. Nature ecology & evolution, 1-10.

Rosenzweig, M. L. (1995). Species diversity in space and time. Cambridge University Press.

Ruhm, C. J. (2000). Are recessions good for your health?. The Quarterly Journal of economics, 115(2), 617-650.

Salje, H., Kiem, C.T., Lefrancq, N., Courtejoie, N., Bosetti, P., Paireau, J., Andronico, A., Hozé, N., Richet, J., Dubost, C.L. and Le Strat, Y., 2020. Estimating the burden of SARS-CoV-2 in France. Science, 369(6500):208-211.

Sands, P., El Turabi, A., Saynisch, P. A., & Dzau, V. J. (2016). Assessment of economic vulnerability to infectious disease crises. The Lancet, 388(10058), 2443-2448.

Smith, K. F., Goldberg, M., Rosenthal, S., Carlson, L., Chen, J., Chen, C., & Ramachandran, S. (2014). Global rise in human infectious disease outbreaks. Journal of the Royal Society Interface, 11(101), 20140950

Stevens, A. H., Miller, D. L., Page, M. E., and Filipski, M. (2015). The best of times, the worst of times: understanding pro-cyclical mortality. American Economic Journal: Economic Policy, 7(4), 279-311.

Svensson, L. E. O. (1989). Portfolio choice with non-expected utility in continuous time. Economics Letters, 30(4), 313-317.

Tatem, A. J., Rogers, D. J., and Hay, S. I. (2006). Global transport networks and infectious disease spread. Advances in parasitology, 62, 293-343.

Thunström, L, Newbold, S. C., Finnoff, D., Ashworth, M. and Shogren, J. F. (2020), The benefits and costs of using social distancing to flatten the curve for COVID-19. Journal of Benefit Cost Analysis, 1-17.

Wolfe N. D., Daszak P., Kilpatrick A. M. and Burke D. S. (2005). Bushmeat hunting, deforestation, and prediction of zoonoses emergence. Emerging infectious diseases, 11(12), 1822-7.

Wood, C. L., McInturff A., Young H. S., Kim D. and Lafferty K. D. (2017). Human infectious disease burdens decrease with urbanization but not with biodiversityPhil. Trans. R. Soc. B37220160122 http://doi.org/10.1098/rstb.2016.0122

World Bank (2014), The economic impact of the 2014 Ebola epidemic: Short and medium term estimates for West Africa.

World Bank (2020), Poverty and Distributional Impacts of COVID-19: Potential Channels of Impact and Mitigating Policies.

Appendix A. Proofs of Lemmas 2.1 and 2.2

Proof of Lemma 2.1. Using per-capita variables $s = \frac{S}{N}$ and $i = \frac{I}{N}$, system (3) reads

$$\left\{ \begin{array}{l} \frac{dN(t')}{dt'} = (n - \delta i\,(t'))\,N\,(t') \\ \frac{ds(t')}{dt'} = \nu\,(1 - s(t')) - \beta s(t')i(t') + \delta s(t')i(t') \\ \frac{di(t')}{dt'} = \beta s(t')i(t') - (\delta + r + \nu)\,i(t') + \delta i(t')^2 \end{array} \right. \tag{17}$$

To study this dynamics, we need to take into account the orders of magnitude of the parameters. According to the data, the growth rate n, birth rate ν and mortality rate μ of the population are small compared to the virus-induced mortality rate δ, which is small compared to the other parameters of the epidemics β and r.

We thus rewrite $n = \varepsilon\eta\widetilde{n}$, $\nu = \varepsilon\eta\widetilde{\nu}$, $\mu = \varepsilon\eta\widetilde{\mu}$, and $\delta = \eta\widetilde{\delta}$, where $0 < \eta << 1$ and $0 < \varepsilon << 1$. Now parameters $\widetilde{n}$, $\widetilde{\nu}$, $\widetilde{\mu}$ and $\widetilde{\delta}$ are of the same order of magnitude. We also consider three time scales: a fast time scale t', an intermediate time scale σ and a slow time scale t, defined as $t = \varepsilon\eta t'$ and $t = \eta\sigma$.

Step 1 of the proof

Introducing the change of variable $y = i/\varepsilon$ and skipping the time variable, system (17) can be written as:

$$\left\{ \begin{array}{l} \frac{dN(t')}{dt'} = \varepsilon\eta\left(\widetilde{n} - \widetilde{\delta}y\right)N \\ \frac{ds(t')}{dt'} = \varepsilon\eta\left(\widetilde{\nu}(1-s) + \widetilde{\delta}sy\right) - \varepsilon\beta sy \\ \frac{dy(t')}{dt'} = \left(\beta s - \eta\widetilde{\delta} - r - \varepsilon\eta\widetilde{\nu} + \varepsilon\eta\widetilde{\delta}y\right)y \end{array} \right. \tag{18}$$

Setting $\varepsilon = 0$ enables to consider system (18) as a regular perturbation of the unperturbed system (19) given by:

$$\left\{ \begin{array}{l} \frac{dN(t')}{dt'} = 0 \\ \frac{ds(t')}{dt'} = 0 \\ \frac{dy(t')}{dt'} = (\beta s - (r + \delta))\,y \end{array} \right. \tag{19}$$

The informations conveyed by system (19) are the following. At fast time, the system expressed in variables (N, s, y) is such that only the y dynamics matters. At this time scale, with this choice of variables, s and N are quite constant. Let $s = s_j$ the constant value of s. Manifold $y = 0$ (called in the following the slow manifold, because it would be the locus of the motion in slow time) is attractive if $s_j < \frac{r+\delta}{\beta} = \frac{1}{R_0}$, where R_0 is the reproduction ratio of the disease. This slow manifold is also called the disease-free equilibrium. According to Tikhonov's theorem, a trajectory of system (18) satisfying $s_j < \frac{1}{R_0}$, quickly jumps to the slow manifold $y = 0$, where the slow motion takes place.

Step 2 of the proof

We now consider the slow motion of system (18) on the slow manifold $y = 0$. To do so, let us write system (18) using slow time t:

$$\left\{\begin{array}{l} \frac{dN(t)}{dt} = \left(\widetilde{n} - \widetilde{\delta} y\right) N(t) \\ \eta \frac{ds(t)}{dt} = \eta\left(\widetilde{\nu}(1-s) + \widetilde{\delta} s y\right) - \beta s y \\ \varepsilon\eta \frac{dy(t)}{dt} = \left(\beta s - \eta\widetilde{\delta} - r - \varepsilon\eta\widetilde{\nu} + \varepsilon\eta\widetilde{\delta} y\right) y \end{array}\right. \tag{20}$$

Setting $\varepsilon = 0$ and $\eta = 0$ enables to consider system (20) as a singular perturbation of the unperturbed system (21) given by:

$$\left\{\begin{array}{l} \frac{dN(t)}{dt} = \left(\widetilde{n} - \widetilde{\delta} y\right) N(t) \\ 0 = -\beta s y \\ 0 = (\beta s - r) y \end{array}\right. \tag{21}$$

On the slow manifold, the dynamics satisfies $\frac{dN(t)}{dt} = \widetilde{n} N(t)$. Thus the growth rate of the population is constant. It will remain constant until the slow manifold becomes unstable or a new epidemic outbreak occurs.

Step 3 of the proof

It now remains to explain why there exists s_j such that the slow manifold is attractive. To do this, let us come back to the original fast time scale system (17). Setting $\varepsilon = 0$ and $\eta = 0$ enables to consider this system as a regular perturbation of the unperturbed system (22) given by:

$$\left\{\begin{array}{l} \frac{dN(t')}{dt'} = 0 \\ \frac{ds(t')}{dt'} = -\beta s i \\ \frac{di(t')}{dt'} = \beta s i - r i \end{array}\right. \tag{22}$$

First integral of the system can be used to compute the final size of the epidemics, which is defined as the number s_∞ of per capita susceptibles at the end of the epidemic outbreak. s_∞ is solution of the following equation:

$$s_\infty - \frac{r}{\beta} \ln s_\infty = 1 + i_0$$

As $r/\beta \simeq 1/R_0$ since δ is very small compared to r and β, this equation can also be written on the more standard following form:

$$s_\infty - \frac{1}{R_0} \ln s_\infty = 1 + i_0 \tag{23}$$

The share of the population $1 - s_\infty$ that has been infected is either recovered or dead. The per capita number of deaths is then $\frac{\delta}{r+\delta}(1 - s_\infty)$. Thus the final size if the

population after the fast epidemic outbreak is $kN(t_j)$, with

$$k = 1 - \frac{\delta}{r+\delta}(1 - s_\infty) \tag{24}$$

Moreover, as $ds(t')/dt' < 0$, there exists an instant t"such that $s(t") = s_j < \frac{1}{R_0}$. Thus according to step 2 the dynamics quickly jumps to the slow manifold, where the slow motion then takes place. □

Proof of Lemma 2.2. In the case where the transmission rate is an increasing function of the intensity of social interactions, $\beta(e)$, with $\beta'(e) > 0$, the reproduction number $R_0 = \frac{\beta}{r+\delta}$ is an increasing function of e as well, and the implicit function theorem, applied to equation (23) yields:

$$\frac{ds_\infty}{de} = -R_0'(e)\frac{s_\infty(1 + i_0 - s_\infty)}{1 - R_0(e)s_\infty}$$

which is negative as soon as $s_\infty < \frac{1}{R_0}$, which is the case. Thus, according to equation (24),

$$\frac{dk}{de} = \frac{\delta}{r+\delta}\frac{ds_\infty}{de} < 0$$

□

Appendix B. Proofs of Theorem 3.1 and Proposition 3.2

Proof of Theorem 3.1. As already mentioned in the main text the HJB equation related to our maximization problem is

$$\begin{aligned}\rho\frac{1-\theta}{1-\phi}V(A,N) = \max_{v,e}\Bigg[&N^\lambda\frac{[(1-f)A]^{1-\phi}}{1-\phi}\frac{1}{((1-\theta)V(A,N))^{\frac{1-\phi}{1-\theta}-1}} \\ &+ V_A gA + V_N nN + \varepsilon(1-f)\left(V(\kappa(e)A, k(e)N) - V(A,N)\right)\Bigg]\end{aligned} \tag{25}$$

Denote $\tilde{V} = V(\tilde{A}, \tilde{N})$. The optimality condition w.r.t. f yields:

$$1 - f = \left(\frac{N^\lambda A^{1-\phi}}{\varepsilon(V - \tilde{V})((1-\theta)V)^{\frac{1-\phi}{1-\theta}-1}}\right)^{1/\phi} \tag{26}$$

Replacing $1-f$ in the HJB equation (9) yields:

$$\begin{aligned}(27)\quad \rho\frac{1-\theta}{1-\phi}V &= \max_e \frac{N^\lambda A^{1-\phi}}{1-\phi}\left(\frac{N^\lambda A^{1-\phi}}{\varepsilon(V-\tilde{V})((1-\theta)V)^{\frac{1-\phi}{1-\theta}-1}}\right)^{\frac{1-\phi}{\phi}}\frac{1}{((1-\theta)V)^{\frac{1-\phi}{1-\theta}-1}}\\ &\quad + V_A gA + V_N nN + \left(\frac{N^\lambda A^{1-\phi}}{\varepsilon(V-\tilde{V})((1-\theta)V)^{\frac{1-\phi}{1-\theta}-1}}\right)^{1/\phi}\varepsilon(\tilde{V}-V)\\ &= \max_e \frac{\phi}{1-\phi}\left(N^\lambda A^{1-\phi}\right)^{\frac{1}{\phi}}\left(\varepsilon(V-\tilde{V})\right)^{-\frac{1-\phi}{\phi}}\left(((1-\theta)V)^{\frac{1-\phi}{1-\theta}-1}\right)^{-\frac{1}{\phi}} + V_A gA + V_N nN\end{aligned}$$

We try to find a solution of the form:

$$V(A,N) = X\frac{N^\alpha A^{1-\theta}}{1-\theta}.$$

for some real positive parameters α and X. In this case

$$\begin{aligned}\tilde{V} &= k(e)^\alpha \kappa(e)^{1-\theta}V\\ V_A &= (1-\theta)\frac{V}{A}\\ V_N &= \alpha\frac{V}{N}\end{aligned}$$

Using these expressions in the HJB equation above we get:

$$\begin{aligned}\rho\frac{1-\theta}{1-\phi}V &= \max_e \frac{\phi}{1-\phi}\left(N^\lambda A^{1-\phi}\right)^{\frac{1}{\phi}}\left[\varepsilon(1-k(e)^\alpha\kappa(e)^{1-\theta})V\right]^{-\frac{1-\phi}{\phi}}\left(((1-\theta)V)^{\frac{1-\phi}{1-\theta}-1}\right)^{-\frac{1}{\phi}}\\ &\quad + (1-\theta)gV + \alpha nV\end{aligned}$$

i.e.

$$\begin{aligned}&\rho\frac{1}{1-\phi} - g - \frac{\alpha}{1-\theta}n\\ &= \max_e \frac{\phi}{1-\phi}\left(N^\lambda A^{1-\phi}\right)^{\frac{1}{\phi}}\left[\frac{\varepsilon\left(1-k(e)^\alpha\kappa(e)^{1-\theta}\right)}{1-\theta}\right]^{-\frac{1-\phi}{\phi}}\left(N^\alpha A^{1-\theta}\right)^{-\frac{1}{\phi}\frac{1-\phi}{1-\theta}}X^{-\frac{1}{\phi}\frac{1-\phi}{1-\theta}}\end{aligned}$$

The maximum point for e is given by e^* which maximizes (10). Choosing

$$\alpha = \lambda\frac{1-\theta}{1-\phi}$$

allows us to obtain:

$$\frac{1}{1-\phi}\left(\rho-(1-\phi)g-\lambda n\right) = \frac{\phi}{1-\phi}\left[\frac{\varepsilon\left(1-k(e^*)^\alpha\kappa(e^*)^{1-\theta}\right)}{1-\theta}\right]^{-\frac{1-\phi}{\phi}}X^{-\frac{1}{\phi}\frac{1-\phi}{1-\theta}}$$

i.e. finally (recall that assumption (11) implies $\rho-(1-\phi)g-\lambda n>0$):

$$X=\left(\frac{\phi\left[\frac{\varepsilon\left(1-k(e^*)^\alpha\kappa(e^*)^{1-\theta}\right)}{1-\theta}\right]^{-\frac{1-\phi}{\phi}}}{\rho-(1-\phi)g-\lambda n}\right)^{\phi\frac{1-\theta}{1-\phi}}$$

Then (26) reads:

$$1-f=\left(\frac{1-\theta}{\varepsilon\left(1-k(e^*)^\alpha\kappa(e^*)^{1-\theta}\right)X^{\frac{1-\phi}{1-\theta}}}\right)^{1/\phi}=\frac{(1-\theta)(\rho-(1-\phi)g-\lambda n)}{\phi\varepsilon\left[1-\left(k(e^*)^{\frac{\lambda}{1-\phi}}\kappa(e^*)\right)^{1-\theta}\right]} \tag{28}$$

Since condition (11) is verified this value is in $(0,1)$.

We finally compute the transversality condition. We need to obtain that

$$\lim_{t\to\infty}e^{-\rho t}\mathbb{E}V(A(t),N(t))=0.$$

The optimal evolution of $A(t)$ and $N(t)$ are

$$\begin{aligned}A(t)&=A_0e^{gt}\kappa(e^*)^{q(t)-q(0)}\\N(t)&=N_0e^{nt}k(e^*)^{q(t)-q(0)}\end{aligned}$$

Then:

$$V(A(t),N(t))=\frac{X}{1-\theta}N_0^{\lambda\frac{1-\theta}{1-\phi}}A_0^{1-\theta}e^{\left((1-\theta)g+\lambda\frac{1-\theta}{1-\phi}n\right)t}\kappa(e^*)^{(1-\theta)(q(t)-q(0)}k(e^*)^{\lambda\frac{1-\theta}{1-\phi}(q(t)-q(0)}$$

and

$$\mathbb{E}\left[\frac{(1-\theta)\,V\left(A(t),N(t)\right)}{XN_0^{\lambda\frac{1-\theta}{1-\phi}}A_0^{1-\theta}}\right]=e^{\left((1-\theta)g+\lambda\frac{1-\theta}{1-\phi}n-\left(1-\kappa(e^*)^{1-\theta}k(e^*)^{\lambda\frac{1-\theta}{1-\phi}}\right)\varepsilon(1-f^*)\right)t}$$

i.e., using the definition of f^*,

$$\mathbb{E}\left[\frac{(1-\theta)\,V\left(A(t),N(t)\right)}{XN_0^{\lambda\frac{1-\theta}{1-\phi}}A_0^{1-\theta}}\right]=e^{\left((1-\theta)g+\lambda\frac{1-\theta}{1-\phi}n-\frac{1-\theta}{\phi}(\rho-(1-\phi)g-\lambda n)\right)t}$$

So we have $e^{-\rho t}\mathbb{E}V(A(t),N(t))\to 0$ as far as

$$-\rho+\left((1-\theta)g+\lambda\frac{1-\theta}{1-\phi}n-\frac{1-\theta}{\phi}(\rho-(1-\phi)g-\lambda n)\right)<0$$

which reduces to the condition asked in (12). □

Proof of Proposition 3.2. In the case of an interior solution on f^*, equation (13) reads:

$$f^* = 1 - \frac{\rho - (1-\phi)g - \lambda n}{\varepsilon\phi} \frac{1-\theta}{1 - z(e^*)^{1-\theta}}$$

with

$$z(e^*) = k(e^*)^{\frac{\lambda}{1-\phi}} \kappa(e^*)$$

and e^* does not depend on θ. Then

$$\frac{\partial f^*}{\partial \theta} = \frac{(\rho - (1-\phi)g - \lambda n)[1 - (1 - (1-\theta)\ln z(e^*))z(e^*)^{1-\theta}]}{\varepsilon\phi(1 - z(e^*)^{1-\theta})^2}$$

$$\frac{\partial f^*}{\partial \theta} \geq 0 \iff 1-(1-(1-\theta)\ln z(e^*))z(e^*)^{1-\theta} \geq 0 \iff (1-(1-\theta)\ln z(e^*))z(e^*)^{1-\theta} \leq 1.$$

Let $P(\theta) = (1 - (1-\theta)\ln z)z^{1-\theta}$.

$$P'(\theta) = \ln z z^{1-\theta} + (1 - (1-\theta)\ln z)\frac{\partial e^{(1-\theta)\ln z}}{\partial \theta} = (1-\theta)(\ln z)^2 z^{1-\theta}.$$

$$P'(\theta) \gtreqless 0 \iff \theta \lesseqgtr 1.$$

P is therefore maximum for $\theta = 1$, and as $P(1) = 1$ we can conclude that indeed $P(\theta) \leq 1$. f^* is an increasing function of θ.

Regarding the dependence of f^* on λ, we have:

$$\frac{\partial f^*}{\partial \lambda} = \underbrace{\frac{1}{\varepsilon\phi}\frac{1-\theta}{1 - z(e^*)^{1-\theta}}}_{>0} \left[n - \underbrace{(\rho - (1-\phi)g - \lambda n)\frac{(1-\theta)z(e^*)^{-\theta}}{1 - z(e^*)^{1-\theta}}}_{>0} \frac{\partial z(e^*)}{\partial \lambda} \right]$$

$$\frac{\partial z(e^*)}{\partial \lambda} = z(e^*)\left[\frac{1}{1-\phi}\ln k(e^*) + \left(\frac{\lambda}{1-\phi}\frac{k(e^*)'}{k(e^*)} + \frac{\kappa(e^*)'}{\kappa(e^*)}\right)\frac{\partial e^*}{\partial \lambda}\right]$$

According to the optimality condition defining the mitigation policy (equation (15)) the term in parenthesis on the right-hand side member of this equation is nil. Then

$$\frac{\partial z(e^*)}{\partial \lambda} = z(e^*)\frac{1}{1-\phi}\ln k(e^*) < 0,$$

from which we conclude that $\frac{\partial f^*}{\partial \lambda} > 0$.

Finally, regarding the dependence of f^* on ϕ, we have:

$$\frac{\partial f^*}{\partial \phi} = \underbrace{\frac{1}{\varepsilon\phi}\frac{1-\theta}{1 - z(e^*)^{1-\theta}}}_{>0} \left[\frac{\rho - g - \lambda n}{\phi} - \underbrace{(\rho - (1-\phi)g - \lambda n)\frac{(1-\theta)z(e^*)^{-\theta}}{1 - z(e^*)^{1-\theta}}}_{>0} \frac{\partial z(e^*)}{\partial \lambda} \right]$$

with

$$\frac{\partial z(e^*)}{\partial \phi} = z(e^*)\frac{1}{(1-\phi)^2}\ln k(e^*) < 0.$$

The sign of $\frac{\partial f^*}{\partial \phi}$ is therefore ambiguous. A sufficient condition for it to be positive is $\rho \geq g + \lambda n$, that is a high enough discount rate. □

Acknowledgements

The work of Giorgio Fabbri is supported by the French National Research Agency in the framework of the "Investissements d'avenir" program (ANR-15-IDEX-02) and of the center of excellence LABEX MME-DII (ANR-11-LBX-0023-01)

Emmanuelle Augeraud-Véron, GREThA, Université de Bordeaux, France
Email address: emmanuelle.augeraud@u-bordeaux.fr

Giorgio Fabbri, Univ. Grenoble Alpes, CNRS, INRAE, Grenoble INP, GAEL, Grenoble, France.
Email address: giorgio.fabbri@univ-grenoble-alpes.fr

Katheline Schubert, Paris School of Economics, Université Paris 1 Panthéon-Sorbonne, France.
Email address: schubert@univ-paris1.fr